Int J Adv Manuf Technol (2016) 87:801–809
DOI 10.1007/s00170-016-8523-6

ORIGINAL ARTICLE

Chatter reliability of milling system based on first-order second-moment method

Yu Liu[1] · **Lin-lin Meng**[1] · **Kuo Liu**[2] · **Yi-min Zhang**[1]

Received: 6 November 2015 / Accepted: 17 February 2016 / Published online: 1 March 2016

Abstract In this paper, reliability analysis for dynamic structural system is presented to predict chatter vibration in a milling system. Chatter reliability is defined to represent the probability of stability (no chatter occurs) of milling system. Probability model (reliability model) of chatter vibration is established to predict milling chatter vibration, in which structural parameters and spindle speed are considered as random variables. Choosing chatter frequency as an intermediate variable, the reliability model is built. The first-order second-moment method is adopted to solve the reliability model of the milling process system to obtain the reliability level of the system. The reliability lobe diagram (RLD), which is a contour line with a specified reliability level as a function of spindle speed and cutting depth, is presented to designate the reliable region for chatter vibration prediction. A numerical example is used to demonstrate the method for reliability analysis. The reliability of milling chatter system was calculated using first-order second-moment (FOSM) method and compared to the Monte Carlo simulation method. The results from the FOSM method and Monte Carlo method were found to be similar. Comparing the results with the traditional stability lobe digram (SLD) method, chatter reliability of milling process system can be used to judge the probability of stability of milling process system. It can be concluded that RLD can be efficiently used to predict reliability in workshop applications.

Keywords Milling process · Chatter reliability · First-order second-moment · Reliability lobe diagram

✉ Yu Liu
yuliu@me.neu.edu.cn

Lin-lin Meng
mlldbdx@163.com

Kuo Liu
kuo_liu@smtcl.com

Yi-min Zhang
ymzhang@me.neu.edu.cn

[1] School of Mechanical Engineering and Automation, Northeastern University, Shenyang, China

[2] State Key Laboratory of Advanced Numerical Control Machine Tool, Shenyang Machine Tool (Group) Co., Ltd, Shenyang, China

1 Introduction

Regenerative chatter in machining operations such as milling is a type of self-excited vibration with a time-delayed displacement feedback mechanism. The most important characteristic of chatter vibration is that it is induced and maintained by the vibrations resulting from the dynamic cutting process rather than external periodic forces. Numerous problems such as poor surface finish, excessive noise, breakage of machine tool components, and reducing tool life and productivity often associated with chatter vibration. Extensive researches focusing on preventing regenerative chatter by predicting its occurrence [1–4], improving detecting methods, or by reducing chatter vibrations with active or passive control strategies [5–8] have been reported in literature. However, chatter is still among the most complicated problems faced by the machinist.

Tobias and Fishwick were the first to propose that chatter vibration stems from the instability of the machining system. They used an orthogonal cutting model to analyze milling stability and validate their hypothesis. One method to predict and avoid pre-process chatter is the well-known stability lobe diagram (SLD). SLD identifies stable and unstable cutting zones by axial depth in milling and spindle speed. Budak et al. [9] developed a method to

analytically determine the stability lobes directly in the frequency domain. This method is known as zero-order approximation. To improve prediction accuracy, Budak and Altintas suggested a higher-order model to predict the stability of cutting process. However, Insperger et al. [10–12] employed the semi-discretization scheme to solve stability in discrete time domain. Ding et al. [13–15] proposed a full-discretization method to obtain SLD in time domain. Besides, Schmitz et al. [16] obtained SLD by sweeping frequency, where the real part of frequency response function (FRF) of the tool point dynamics is less than zero.

The FRF of the tool point is necessary when the stability of the milling process is analyzed using any of the above methods. The structural parameters of dynamic FRF are typically obtained using impact testing at the tool point.

The result of a measurement is only an approximation or estimation of the specific measurand value, and errors induced in measurements may cause a large error in the stability of milling process. Therefore, it is necessary to study the probability of occurrence of chatter vibrations considering the structural parameters as random variables and provide a new methodology to identify chatter and no chatter cutting zones instead of SLD.

Random structural system reliability analysis is a method that introduces probability analysis and design into structural analysis of random variables. Until recently, studies of reliability analysis including static and dynamic structural systems have made much progress. The issue of reliability for dynamic structural systems primarily includes two aspects: the first is the structural response (displacement, stress, etc.) overrun caused by forced vibration [17, 18]; the second is the fatigue caused by resonant and non-resonant structures [19]. Liu [] proposed a probability method for the single degree of freedom (DOF) orthogonal turning in which the failure condition is defined as losing the system stability. The two DOF milling process systems have a complicated dynamic model. The study of the reliability of a dynamic structural system on the instability of self-excited vibration due to time-delay, e.g. regenerative chatter of milling process, has not been reported in literature and needs to be investigated.

This paper introduces the idea of reliability analysis in dynamic structural systems into structural analysis of the milling process. Here, chatter reliability is defined as the probability of stability when no chatter occurs in the milling process system. The chatter probability model is established to predict milling chatter vibration, in which structural parameters modal mass m, modal damping c, modal stiffness k, and spindle speed Ω are random variables. Choosing chatter frequency Ω_c as an intermediate variable, reliability model is built. The second-moment method was adopted to solve the milling process system reliability model and obtain the reliability level of the system.

2 Dynamic model of milling process system

2.1 Milling system

A typical milling system consists of a spindle, milling tool, and the workpiece. Generally, the cutter is relatively flexible, whereas, the workpiece is rigid. The schematic diagram of milling process system is shown in Fig. 1. The cutter is assumed to have N number of teeth with a zero helix angle. The flexibility of the cutter is represented by a two degree-of-freedom system in the x and y directions. The cutting forces excite the structure to vibration in the x and y directions, causing dynamic displacements x and y, respectively.

The milling system is a typical time-delayed displacement feedback system in which the force is a function of the vibration displacement in the current cycle and one-tooth delayed cycle.

2.2 Dynamic force of milling process

As shown in Fig. 1, the angle between the dynamic milling force F and normal direction at the cutting point is β; the angle between the normal direction at the cutting point and y-axis is ϕ (cutting angle). The dynamic force of the milling system is given as

$$F(t) = K_s b h(t) \tag{1}$$

where $F(t)$ is the dynamic cutting force(in N), K_s is the cutting stiffness coefficient (in N/m^2), b is the cutting depth (in m) and $h(t)$ is the instantaneous chip thickness between the current and previous cycles. The instantaneous chip thickness in milling can be written as

$$h(t) = f_t \sin(\phi) + n(t-\tau) - n(t) \tag{2}$$

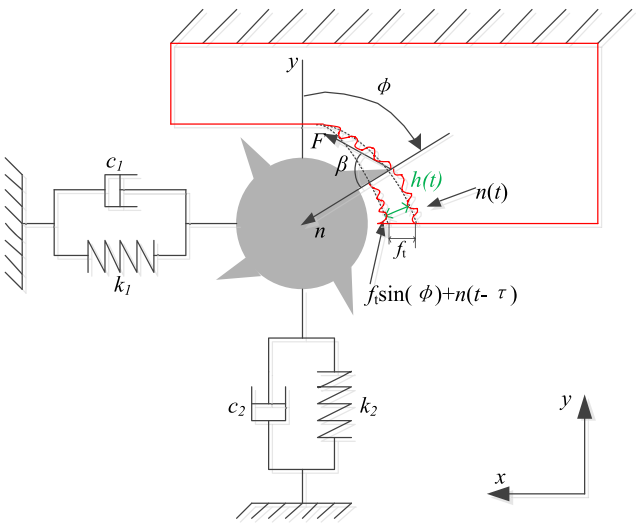

Fig. 1 Schematic diagram of a typical milling process

where f_t is the feed per tooth and $f_t \sin(\phi)$ is the static component of the chip thickness. The difference between $n(t-\tau)$ and $n(t)$ is the dynamic component of the chip thickness along the normal direction by the previous tooth, t is the time variable, τ is the delayed time between two teeth, and $\tau = 60/\Omega N_t$, where Ω is given in rpm.

2.3 Oriented frequency response function

The oriented frequency response function (FRF) is calculated by summing the products of the directional orientation factors and corresponding FRFs for the x and y directions.

$$\mathrm{FRF_o} = \mu_x \mathrm{FRF}_x + \mu_y \mathrm{FRF}_y \tag{3}$$

where, μ_x and μ_y are directional orientation factors for x- and y-axis, respectively, and FRF_x and FRF_y are the FRF for x and y directions, respectively. FRF_o is the FRF oriented in the average surface normal direction. The average surface normal direction is defined as the normal of the cutting path at the average cutting angle, and the average cutting angle is defined as Eq. (4). Figure 2 shows the geometry in up and down milling, where the ϕ_s and ϕ_e are the start and exit angles of the tooth, respectively, and ϕ_{avg} is the average cutting angle. The start angle in up milling is $\varphi_s = 0$, while the exit angle, φ_e, depends on the radial depth of cut, a, and tool radius r. The exit angle in down milling is $\varphi_e = 0$, while the start angle, φ_s, depends on the radial depth of cut, a, and tool radius r.

$$\phi_{avg} = \frac{\phi_e - \phi_s}{2} \tag{4}$$

Two steps are required to determine the directional orientation factors along the x and y directions. First, the force is projected onto the x- and y-axis. Second, this result is projected onto the surface normal. Since, the oriented FRF is the linear superposition of the FRFs for x and y direction and the latter is commonly obtained by the hammer test, we can write the oriented FRF according to a single DOF dynamic system as follows:

$$\mathrm{FRF_o} = \frac{1}{k\left(\frac{(j\omega)^2}{\omega_n^2} + \frac{2\zeta\omega}{\omega_n} j + 1\right)} \tag{5}$$

$$\omega_n^2 = \frac{k}{m} \tag{6}$$

$$\zeta = c \Big/ \left(2\sqrt{mk}\right) \tag{7}$$

where m, c, k, Ω_n, and ζ, respectively, represent the equivalent mass, equivalent damping, equivalent stiffness, natural frequency, and equivalent damping ratio of the vibration system in the normal direction at average cutting angle.

Separating the real and imaginary parts from Eq. (5), we obtain

$$Re(\mathrm{FRF}_o) = \frac{1}{k}\left(\frac{1-r^2}{(1-r^2)^2 + (2\zeta r)^2}\right) \tag{8}$$

$$Im(\mathrm{FRF}_o) = \frac{1}{k}\left(\frac{-2\zeta r}{(1-r^2) + (2\zeta r)^2}\right) \tag{9}$$

where r is the ratio of Ω by Ω_n.

2.4 Stability lobes diagram

The limiting cutting depth b_{lim} of the milling process system is as follows:

$$b_{lim} = \frac{-1}{2K_s Re[\mathrm{FRF}_o] N_t^*} \tag{10}$$

$$N_{t^*} = \frac{\phi e - \phi s}{360 \Big/ N_t} \tag{11}$$

$$\frac{\frac{\omega_c}{2\pi}}{\Omega N_t} = N + \frac{\varepsilon}{2\pi} \tag{12}$$

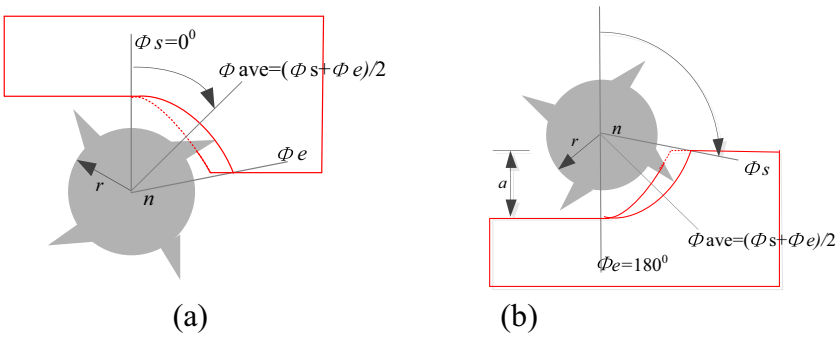

Fig. 2 Average cut angle ϕ_{avg}, **a** up milling and **b** down milling

$$\varepsilon = 2\pi - 2\tan^{-1}\left(\frac{Re[\mathrm{FRF_o}]}{Im[\mathrm{FRF_o}]}\right) \tag{13}$$

Where, N_t^* represents the average number of teeth in the cutter. N_t is the number of teeth on the cutter. Equation (7) relates the chatter frequency, Ω_c (in rad/s), should it occur, to spindle speed, Ω (rev/s), so that the stability lobe diagram may be plotted. In Eq. (12), $N=0$, 1, 2, is the integer number of vibration waves between tooth (lobe number) and ε (in rad) and is defined in Eq. (13).

3 Milling chatter reliability model

3.1 Random variables of the system

Chatter occurs in the milling process due to the interaction between the tool and workpiece. The probability that the chatter vibration will occur is closely related to the structural parameters of the tool point FRF. The basic random variables of milling process system are m, c, k, and Ω, in which m, c, and k represent the structural parameters of the cutter and Ω represents the spindle speed.

3.2 The reliability model of milling chatter system

The performance function of the milling system taking chatter into account is given as

$$g_X(X) = b_{\lim} - b \tag{14}$$

Where, $b_{\lim}$ and b denote the limiting cutting depth and actual cutting depth, respectively. $\boldsymbol{X}$ is the random vector and $\boldsymbol{X}=(m, c, k, \Omega)^{\mathrm{T}}$.

However, it is hard to express the performance function, $g_X(\boldsymbol{X})$ as a function of $\boldsymbol{X}=(m, c, k, \Omega)^{\mathrm{T}}$, because of the existing of N in Eq. (12). For each vector $\boldsymbol{X}$, there will be N values of g_X. The chatter frequency Ω_c is a non-physical variable. There exits exact one chatter frequency for any spindle speed variable Ω, and we can express the limiting state equation as the function of anew random vector $\boldsymbol{X}_1=(m, c, k, \Omega_c)^{\mathrm{T}}$ as shown in Sections 2.3 and 2.4.

The performance function of milling system is obtained by Eqs. (7), (8), (10), and (14):

$$g_{X_1}(\mathbf{X}) = -\frac{\left(k - m\omega_c^2\right)^2 + c^2\omega_c^2}{2K_s N_t^*\left(k - m\omega_c^2\right)} - b \tag{15}$$

The reliability of the dynamic milling process is the probability that chatter does not occur at a given time and for the given function parameters, then the reliability of the model can be defined as

$$R_s = P\left(g_{X_1}(\mathbf{X}) > 0\right) = \int_{X_{1R}} f_{X_1}(x)dx \tag{16}$$

where $f_{X_1}(x)$ is the joint probability density of random vector and X_{1R} is the safe region of the basic variable space, that is, $g_{X1}(\mathbf{X})>0$ in the X_{1R} region. $P(.)$ is the probability function.

4 Reliability calculations

4.1 Chatter frequency

After the SLD is plotted, a numerical method that is illustrated in flowing sentence is used to calculate the chatter frequency Ω_c. Since we can obtain N values of spindle speed Ω and cutting depth $b_{\lim}$ at a given specific chatter frequency Ω_c and choose the final spindle speed Ω according to the minimum $b_{\lim}$. We obtain a 2D array consist of Ω and Ω_c. The column of Ω is sorted by size, whereas, the column of Ω_c is not continuous. The equal interval interpolation is carried on for the 2D array, and we can obtain the chatter frequency Ω_c from each spindle speed Ω.

4.2 Distribution estimation of chatter frequency

Generally, the structural parameters m, c, and k in the milling system and the processing parameter Ω are normally distributed. In order to calculate the reliability of milling system, the mean value and standard variance of random variables needs to be calculated. From Eq. (12), the chatter frequency is a function of random variables m, c, k, and Ω, and the mean and the variance of each of the parameters are obtained from experimental data. A modal force hammer, an acceleration sensor and a set of data acquisition system are required to get the FRF at tool tip. The parameters m, c, and k are calculated based on the FRF data. We can calculate Ω_c from each sample group. In order to determine the distribution type of the Ω_c, a goodness-of-fit test is needed. (Examples show that the chatter frequency is normally distributed.) We can estimate the overall mean value and variance according to the sample of Ω_c and estimate the correlation coefficients between chatter frequency Ω_c and variables m, c, and k, respectively.

4.3 FOSM method for the milling process system reliability

First-order second-moment (FOSM) method linearizes the limit state function at Taylor expansion points on the failure surface. Reliability evaluation of the milling system is presented and discussed in detail below.

The limit state function for milling system is

$$Z = g_X(\boldsymbol{X}) = 0 \tag{17}$$

The basic random variable $\boldsymbol{X}=(X_1, X_2, X_3, X_4)^{\mathrm{T}}$ are relevant random variables of the normal distribution. X_i $(i=1, 2, 3, 4)$ is m, c, k, and Ω_c, respectively. The basic variables are unrelated each other. However, Ω_c is related to m, c, and k, and the correlation matrix of the milling system is

$$\rho = \begin{pmatrix} 1 & 0 & 0 & \rho_{X_1X_4} \\ 0 & 1 & 0 & \rho_{X_2X_4} \\ 0 & 0 & 1 & \rho_{X_3X_4} \\ \rho_{X_4X_1} & \rho_{X_4X_2} & \rho_{X_4X_3} & 1 \end{pmatrix} \tag{18}$$

where ρ_{XiXj} is the correlation coefficient of variable X_i and X_j.

The standard deviation σ_i $(i=1, 2, 3, 4)$ of each random variable is σ_m, σ_c, σ_k, and $\sigma_{\Omega c}$, respectively, and the covariance matrix of milling system is

$$C = \begin{pmatrix} \sigma_1^2 & 0 & 0 & \rho_{X_1X_4}\sigma_1\sigma_4 \\ 0 & \sigma_2^2 & 0 & \rho_{X_2X_4}\sigma_2\sigma_4 \\ 0 & 0 & \sigma_3^2 & \rho_{X_3X_4}\sigma_3\sigma_4 \\ \rho_{X_4X_1}\sigma_1\sigma_4 & \rho_{X_4X_2}\sigma_2\sigma_4 & \rho_{X_4X_3}\sigma_3\sigma_4 & \sigma_4^2 \end{pmatrix} \tag{19}$$

In Eq. (19), matrix $\boldsymbol{C}$ is a 4×4 symmetric positive definite matrix. The matrix has four real characteristic roots and four linearly uncorrelated and orthogonal characteristic vectors. Assuming that the columns of matrix $\boldsymbol{A}$ are consist of regularization characteristic vectors of $\boldsymbol{C}$. Orthogonal transformation is implemented on vector $\boldsymbol{X}$ which consists of random variables of the system.

$$\boldsymbol{X} = \boldsymbol{AY} \tag{20}$$

$$\boldsymbol{\mu}_Y = \boldsymbol{A}^T\boldsymbol{\mu}_X \tag{21}$$

$$\sigma_Y = \boldsymbol{A}^T\boldsymbol{CA} \tag{22}$$

Limiting state function can be expressed as a function of the uncorrelated normal random variable $\boldsymbol{Y}$:

$$\boldsymbol{Z} = g_X(\boldsymbol{X}) = g_X(\boldsymbol{AY}) \Rightarrow \boldsymbol{Z}_L = g_Y(\boldsymbol{Y}) \tag{23}$$

The derivative of the random variable $\boldsymbol{Y}$ is calculated by using the design point method [21], and its derivative is

$$\frac{\partial g_Y(\boldsymbol{Y})}{\partial Y_i} = A^T\frac{\partial g_X(\boldsymbol{X})}{\partial X_i} \tag{24}$$

Choosing a mean value, $\boldsymbol{X}^*=(m^*, c^*, k^*, \Omega_c^*)$, as the initial design point, thus the initial value of $\boldsymbol{Y}^*$ is:

$$\boldsymbol{Y}^* = \boldsymbol{A}^T\boldsymbol{\mu}_X \tag{25}$$

The partial derivatives of random vector $\boldsymbol{X}$ are as follows

$$\frac{\partial g_X(\boldsymbol{X})}{\partial m} = \frac{\omega_c{}^2\left(-c^2\omega_c{}^2 + k^2 - 2km\omega_c{}^2 + m^2\omega_c{}^4\right)}{2K_sN_t{}^*\left(k-m\omega_c{}^2\right)^2} \tag{26}$$

$$\frac{\partial g_X(\boldsymbol{X})}{\partial c} = -\frac{c\omega_c{}^2}{K_sN_t{}^*\left(k-m\omega_c{}^2\right)} \tag{27}$$

$$\frac{\partial g_X(\boldsymbol{X})}{\partial k} = -\frac{1}{2K_sN_t{}^*} - \frac{c^2\omega_c{}^2}{2K_sN_t{}^*\left(k-m\omega_c{}^2\right)^2} \tag{28}$$

$$\frac{\partial g_X(\boldsymbol{X})}{\partial \omega_c} = \frac{m\omega_c}{K_sN_t{}^*} - \frac{c^2k\omega_c}{K_sN_t{}^*\left(k-m\omega_c{}^2\right)^2} \tag{29}$$

Substituting Eqs. (26), (27), (28), and (29) into Eq. (24), we obtain the derivative of linearly uncorrelated random variables $\boldsymbol{Y}$.

In the space of random variable $\boldsymbol{Y}$, equation $\boldsymbol{Z}_L=0$ is the tangent plane at the point $\boldsymbol{Y}^*$. According to properties of linear combination of the independent random variables of normal distribution, we obtain the mean value and standard deviation of $\boldsymbol{Z}_L$:

$$\mu_{Z_L} = g\left(Y^*\right) + \sum_{i=1}^{4}\frac{\partial g\left(Y^*\right)}{\partial Y_i}\left(\mu_{Y_i} - Y_i^*\right) \tag{30}$$

$$\sigma_{Z_L} = \sqrt{\sum_{i=1}^{4}\left[\frac{\partial g\left(Y^*\right)}{\partial Y_i}\right]^2\sigma_{Y_i}^2} \tag{31}$$

The first-order second-moment mean value reliability index β of the system can be written as

$$\beta = \frac{\mu_{Z_L}}{\sigma_{Z_L}} \tag{32}$$

The sensitivity coefficient of variable Y_i is defined as:

$$\cos\theta_{Y_i} = -\frac{\frac{\partial g\left(Y^*\right)}{\partial Y_i}\sigma_{Y_i}}{\sqrt{\sum_{i=1}^{4}\left[\frac{\partial g\left(Y^*\right)}{\partial Y_i}\sigma_{Y_i}\right]^2}} \tag{33}$$

Thus, the new design point $\boldsymbol{Y}^*$ is

$$Y^* = \mu_{Y_i} + \beta\sigma_{Y_i}\cos\theta_{Y_i} \tag{34}$$

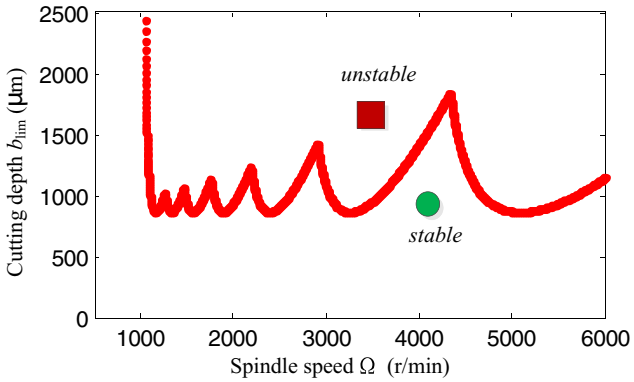

Fig. 3 Example of stability lobe diagram

The new design point in original coordinates $\boldsymbol{X}^*$ is

$$X^* = AY^* \tag{35}$$

Setting the error $\varepsilon = 10^{-6}$, multiple iterations were required until the difference $\|X^*\| < \varepsilon$. The value of β from the computations was substituted into Eq. (32).

Reliability (or reliability probability) of the system is as follows:

$$p_r = 1 - \Phi(-\beta) \tag{36}$$

5 Reliability lobes diagram

Figure 3 shows an example of stability lobe diagram. In the figure, Ω versus b_{lim} family of curves separates the space into two regions. Any (Ω, b) pair that appears above the collective boundary indicates unstable behavior, while any pair below the boundary is presumed to be stable.

In the (Ω, b) plane, the plane can be divided by grids with appropriate increments. The reliability value at the node whose coordinates are (Ω_m, b_n) can be calculated. If the data is sufficient, a contour line can be obtained for the given reliability value p_r^*. The contour plots in the (Ω, b) plane are

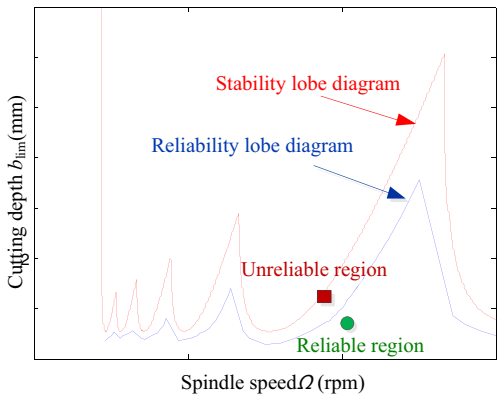

Fig. 4 An example of reliability and stability lobe diagram

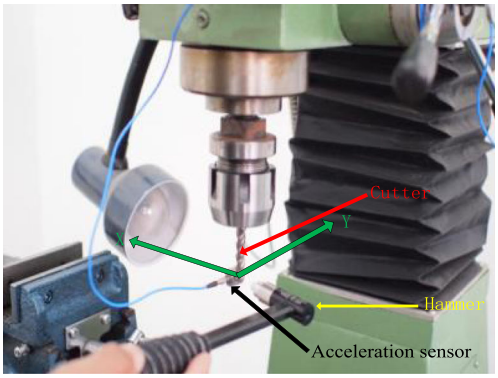

Fig. 5 Experimental setup for dynamic testing of the milling system

defined as reliability lobes diagram, and it is also has a lobe shape. Figure 4 shows an example of reliability lobe diagram.

Compared with the stability lobe diagram, reliability lobe diagram can estimate the reliability at the selected point. There are different reliability requirements in different milling systems in engineering, so the cutting depth and the speed can be selected to meet the requirements from the reliability lobe diagram. As shown in Fig. 4, the red line represents the stability lobe diagram, and the blue line represents the reliability lobe diagram. Any (Ω, b) pair that appears above the blue line indicates unreliable behavior, and the probability of stability (no chatter occurs) is greater than p_r^*. However, any pair below the boundary is presumed to be reliable, and probability of stability (no chatter occurs) is less than p_r^*.

6 A numerical example

A slotting cut was done using vertical milling machine and is used as an example for the analysis discussed in the previous

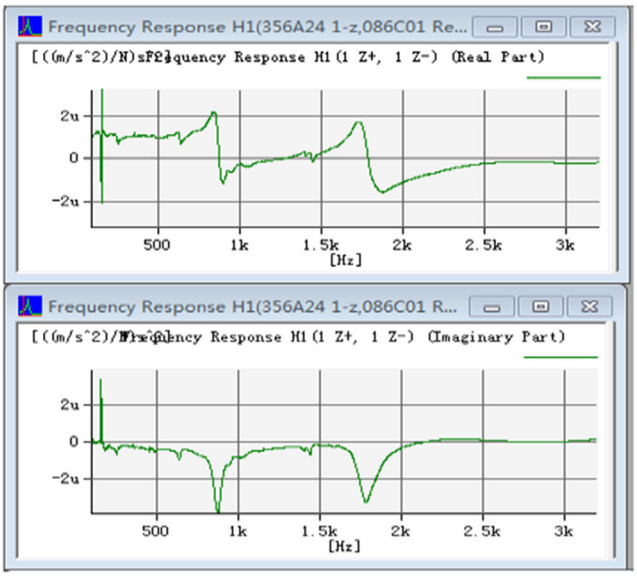

Fig. 6 Tested FRF in X direction for the milling machine tool

Table 1 The parameter values of cutter in *X* direction

	Ω_{nx} (rad/s)	f_{nx} (Hz)	k_x (N/m)	m_x (kg)	c_x (N s/m)
1	5451.04	868	4.20e+06	0.141325	47.03877
2	5463.6	870	4.06e+06	0.135885	47.78838
3	5451.04	868	4.31e+06	0.145044	48.27663
4	5451.04	868	4.40e+06	0.148163	49.31484
5	5451.04	868	4.37e+06	0.147059	48.02388
6	5469.88	871	4.35e+06	0.145309	48.36491
7	5451.04	868	4.27e+06	0.143554	51.38689
8	5488.72	874	4.51e+06	0.149558	49.77919
9	5495	875	4.39e+06	0.145429	49.31805
10	5488.72	874	4.52e+06	0.149968	49.91557

sections. The cutter diameter used here is 14 mm. In the slot milling, the start angle $\phi_s = 0°$, and exit angle $\phi_e = 180°$. Therefore, $\mu_x = \cos\beta$ and $\mu_y = 0$. The related parameters of the milling cutter can be obtained by the frequency response function test. As a result, the reliability of milling process system can be obtained using the FOSM method. The reliability lobe diagram was plotted with the reliability level being 0.99.

6.1 Acquisition and analysis of structural parameters

The test of the FRF at tool point is conducted on a vertical milling machine (Z7030, SMTCL, China). A vibration signal acquisition system (model 3560-B, Brüel & Kjær, Denmark), a pulse analysis software (Brüel & Kjær, Denmark), a modal hammer (Model: 086C01, PCB Inc., USA), and an acceleration sensor (Model: 356A24, PCB Inc., USA) were used for data collection from the milling system.

The frequency response function test was done along the *x* and *y* directions of the tool. The locations of acceleration sensor and hammer tapping are shown in Fig. 5, and the FRF diagram obtained directly from the test system is shown in Fig. 6. The frequency response of the vertical milling machine

Table 2 The parameter values of cutter in *Y* direction

	Ω_{ny} (rad/s)	f_{ny} (Hz)	k_y (N/m)	m_y (kg)	c_y (N s/m)
1	5275.2	840	8.82e+06	0.317010	91.57790
2	5275.2	840	8.82e+06	0.317010	91.57790
3	5275.2	840	9.32e+06	0.334801	96.71748
4	5281.48	841	8.62e+06	0.309197	95.14616
5	5281.48	841	8.10e+06	0.290237	89.31172
6	5287.76	842	8.73e+06	0.312126	94.08756
7	5281.48	841	8.49e+06	0.304543	95.62670
8	5275.2	840	9.22e+06	0.331419	95.74054
9	5275.2	840	9.51e+06	0.341776	98.73243
10	5287.76	842	8.34e+06	0.298158	93.62178

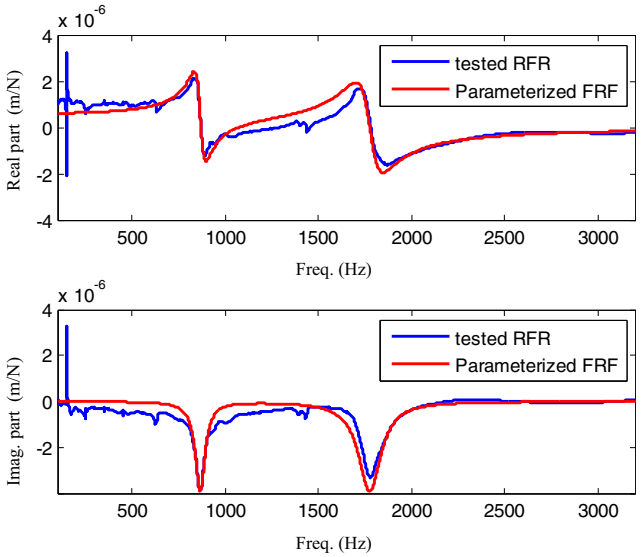

Fig. 7 Comparison of parameterized FRF and tested FRF

tool was obtained using the data acquisition system. Based on the frequency response parameters *m*, *c* and *k*, can be calculated. Data of multiple measurements is shown in Tables 1 and 2. Parameterized FRF using Eqs. (8) and (9) are shown in Fig. 7 for comparison. The second order modal frequency (1785Hz) was high, so it has a small influence on the prediction of chatter vibration. A simplified FRF of only the first modal is adopted to represent the milling process.

The mean values and standard deviations of the structural parameters of the milling process system were calculated, and the results are shown in Table 3. A photoelectric speed sensor was used to measure the speed of spindle and get the deviation of parameters.

6.2 Distribution of chatter frequency

The change of the limiting cutting depth b_{lim} of milling process system and the chatter frequency Ω_c as a function of spindle speed are shown in Fig. 8. The blue line represents the limiting cutting depth, while the red line represents chatter frequency versus the spindle speed.

For a sample size of 10000 of *m*, *c*, *k* and Ω, chatter frequency Ω_c was calculated from Eq. (17). A histogram for different speeds is shown in Fig. 9. When the dynamic parameters *m*, *c*, *k*, and Ω of milling process system are normal

Table 3 The mean and standard deviation of parameters

Direction		f_n (Hz)	*m* (kg)	*c* (N s/m)	*k* (N/m)
X	μ_x	870.4	0.1451	48.92	4.34e6
	σ_x	2.9136	0.0042	1.2682	0.14e6
Y	μ_y	840.7	0.3156	94.21	8.80e6
	σ_y	0.8233	0.0164	2.7924	0.45e6

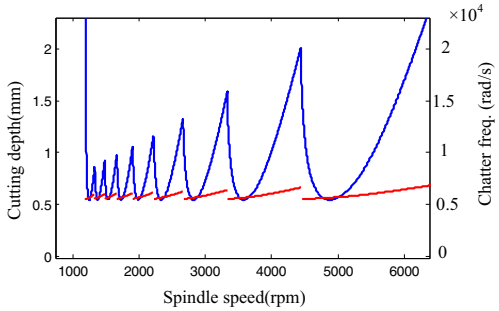

Fig. 8 The lobe diagram and chatter frequency plot of system with mean values

distributed, chatter frequency of the milling system will change in accordance with a certain distribution. The mean values of spindle speed are set to $\Omega = 3000$, 4000, 5500, and 10000 rpm.

For a spindle speed of $\Omega = 10000$ rpm, a Lilliefors goodness-of-fit test was used for the chatter frequency samples. The test results show that the system chatter frequency is normal distributed of a significance level of 95 %. The mean and standard deviation of chatter frequency is Ω_c (6516.6, 24.5593) rad/s. The correlation coefficients of four random variables of the milling system were obtained as follows: the correlation coefficient between m and Ω_c was −0.7635, the correlation coefficient between c and Ω_c was 0.2061, and the correlation coefficient between k and Ω_c was 0.5982.

6.3 Reliability solution

For a spindle speed of 10,000 rpm and a given cutting depth b, the reliability was calculated by the FOSM and Monte Carlo methods and the relative errors of the results of the two methods were calculated, setting ε equal to 10^6. The calculation results are shown in Table 4.

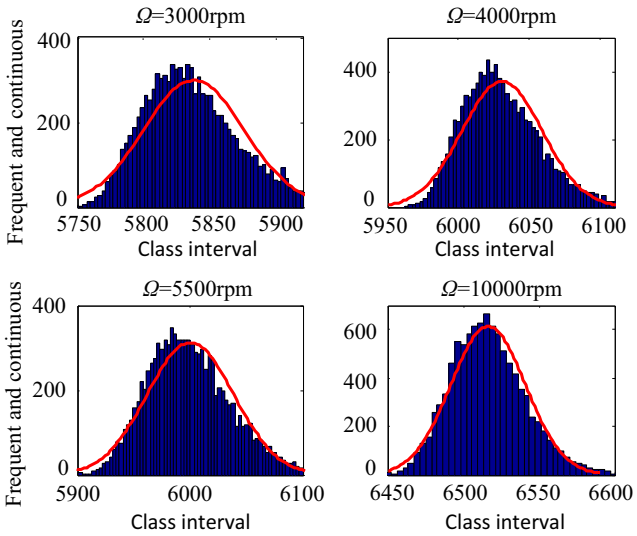

Fig. 9 The distribution histogram of chatter frequency at different spindle speeds

Table 4 The reliability of given depths in a certain spindle speed

b (mm)	P_r (AFOSM)	P_r (Monte Carlo)	Relative error (%)
0.5	1.000000	1.000000	0
0.7	1.000000	1.000000	0
0.9	1.000000	1.000000	0
1.1	0.999990	0.999989	0.0001
1.3	0.998977	0.998929	0.0048
1.5	0.972420	0.972319	0.0104
1.7	0.775198	0.775757	−0.0721
1.9	0.341772	0.341827	−0.0161
2.1	0.057379	0.057205	0.3042
2.3	0.002936	0.002867	2.4067

In Table 4, a million samples were used to calculate the reliability by the Monte Carlo method, that is, the ratio of the number of the case in which the given b is greater than the calculated b_{lim} and the number of total calculation times is considered the result from Monte Carlo method. It can be seen from the table that the results obtained by FOSM and Monte Carlo methods were close; the maximum relative error is 2.4067 %. Therefore, when calculating the reliability of milling chatter system, AFOSM can meet the precision requirements.

6.4 Reliability lobe diagram

The reliability lobe diagram for a reliability value set at 0.99 is shown in Fig. 10 along with the stability lobe diagram shown for comparison. In Fig. 10, the red line represents the stability lobe diagram, and the blue lines represent the reliability lobe diagram with the 0.99 level. Any (Ω, b) pairs below the red line would be stable and those above the red line are unstable. Any (Ω, b) pairs below the blue line are reliable with a level of 0.99. The (Ω, b) pairs located between the red and blue line are stable but unreliable because the reliability is less than the level of 0.99.

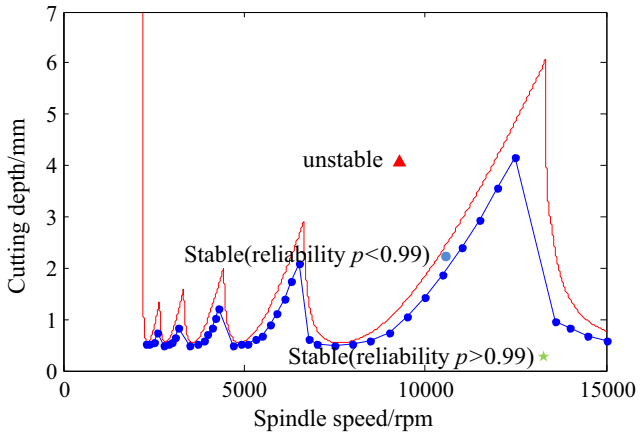

Fig. 10 Reliability lobe diagram

7 Conclusions

The dynamic model of a milling system was established in this paper. In addition, the milling process chatter reliability model with random parameters, FOSM and Monte Carlo method, was presented for the reliability (probability of occurrence of chatter vibrations) of calculation.

The distribution of random parameters for the milling system was measured experimentally, and the lobes diagram and chatter frequency curve of the milling system were shown with mean values of random variables.

The reliability of milling chatter system was calculated using the FOSM method and compared with that calculated by the Monte Carlo method. We can conclude that the relative error between the FOSM and Monte Carlo methods is within 2.4 %. Comparing it with the traditional SLD method, chatter reliability method can be used to judge the probability of stability of milling system. The reliability lobe diagram was used to identify reliable and unreliable cutting zones instead of SLD.

Acknowledgments This work is supported by the Chinese National Natural Science Foundation (51105067, 51135003) and the Fundamental Research Funds for the Central Universities (N120403011).

References

1. Urbikain G, Fernández A, López de Lacalle LN, Gutiérrez ME (2013) Stability lobes for general turning operations with slender tools in the tangential direction. Int J Mach Tools Manuf 67(1):35–44
2. Grossi N, Sallese L, Scippa A, Campatelli G (2014) Chatter stability prediction in milling using speed-varying cutting force coefficients. Proc CIRP 14:170–175
3. Graham E, Mehrpouya M, Nagamune R, Park SS (2014) Robust prediction of chatter stability in micro milling comparing edge theorem and LMI. CIRP J Manuf Sci Technol 7(1):29–39
4. Wang MH, Gao L, Zheng YH (2014) Prediction of regenerative chatter in the high-speed vertical milling of thin-walled workpiece made of titanium alloy. Int J Adv Manuf Technol 72(5):707–716
5. Kakinuma Y, Enomoto K, Hirano T, Ohnishi K (2014) Active chatter suppression in turning by band-limited force control. CIRP Ann Manuf Technol 63(1):365–368
6. Yan Y, Xu J, Wiercigroch M (2015) Non-linear analysis and quench control of chatter in plunge grinding. Int J Non Linear Mech 70: 134–144
7. Monnin J, Kuster F, Wegener K (2014) Control engineering practice optimal control for chatter mitigation in milling—part 1: modeling and control design. Control Eng Pract 24(2):156–166
8. Monnin J, Kuster F, Wegener K (2014) Control engineering practice optimal control for chatter mitigation in milling—part 2: experimental validation. Control Eng Pract 24(2):167–175
9. Budak E, Altintas Y (1995) Analytical prediction of stability lobes in milling. Ann CIRP 44(2):357–362
10. Insperger T, Stépán G (2004) Updated semi-discretization method for periodic delay-differential equations with discrete delay. Int J Numer Methods Eng 61(1):117–141
11. Insperger T, Stépán G (2002) Semi-discretization method for delayed systems. Int J Numer Methods Eng 55(1):503–518
12. Elbeyli O, Sun JQ (2004) On the semi-discretization method for feedback control design of linear systems with time delay. J Sound Vib 273(1–2):429–440
13. Ding Y, Zhu L, Zhang X, Ding H (2010) A full-discretization method for prediction of milling stability. Int J Mach Tools Manuf 50(5): 502–509
14. Ding Y, Zhu L, Zhang X, Ding H (2010) Second-order full-discretization method for milling stability prediction. Int J Mach Tools Manuf 50(10):926–932
15. Huang T, Zhang XM, Zhang XJ, Ding H (2013) An efficient linear approximation of acceleration method for milling stability prediction. Int J Mach Tools Manuf 74(1):56–64
16. Schmitz TL, Smith KS (2009) Machining dynamics-frequency response to improved productivity. Springer Science + Business Media LLC, New York
17. Bergman LA, Heinrich J (1982) On the reliability of the linear oscillator and systems of coupled oscillators. Int J Numer Methods Eng 18(9):1271–1295
18. Spencer BF, Elishakoff I (1988) Reliability of uncertain linear and nonlinear systems. J Eng Mech ASCE 114(1):135–148
19. Zhang YM, Lü CM, Zhou N, Su CQ (2010) Frequency reliability sensitivity for dynamic structural systems. Mech Based Des Struct Mach 38(1):74–85
20. Liu Y, Li TX, Liu K, Zhang YM (2016) Chatter reliability prediction of turning process system with uncertainties. Mech Syst Signal Process 66-67(1):232–247